

General mechanism of optical nonlinearity enhancement by cavity QED

Hisaki Oka,¹ Kazuya Taniguchi,¹ Hiroshi Ajiki,² and Hajime Ishihara¹

¹*Department of Physics and Electronics, Osaka Prefecture University, 1-1 Gakuen-cho, Naka-ku, Sakai 599-8531, Japan*

²*Department of Materials Engineering Science, Osaka University, Toyonaka, Osaka 560-8531, Japan*

(Received 21 October 2008; published 22 December 2008)

The enhancement mechanism of the third-order nonlinear optical response of cavity polaritons is theoretically investigated through the size dependence of the exciton system. Cavity quantum electrodynamics (cavity QED) effect strongly affects the balance between absorption saturation and induced absorption, depending on the system size, through the modification of the level structure of exciton- and biexciton-cavity coupled states. This triggers a drastic change in the optical nonlinearity, which is another essential effect of the cavity QED to enhance the optical nonlinearity.

DOI: 10.1103/PhysRevB.78.245420

PACS number(s): 42.50.Pq, 42.65.-k

I. INTRODUCTION

Nonlinearity control is one of the most essential functions of a cavity system, and the strong-coupling regime realizable in cavity quantum electrodynamics (cavity QED) has produced various nonlinear optical phenomena.¹⁻³ Earlier studies of cavity QED have focused on the coupling of a cavity photon and a first excited state, such as two-level atoms and exciton states in semiconductors, where the main role of the cavity is to amplify the intracavity light field, leading to the enhancement of optical nonlinearity. However, the nonlinearity of such systems decreases with an increase in the system size of N , e.g., the number of atoms, owing to the decrease in anharmonicity.⁴ This becomes a crucial problem in actual experiments conducted with the aim of device applications because it is difficult to accurately control N when it is small. Recently, it has been shown that the size dependence of the nonlinearity of a system with a second excited state such as a biexciton state can remain sufficiently strong even for $N \gg 1$ if the system parameters are carefully designed.⁵ In addition, the application of biexciton-cavity coupling to entangled-photon generation has also been proposed.^{6,7} Thus, the current focus of cavity QED studies is changing from an ideal two-level-like system to a more realistic many-level system with many degrees of freedom.

For a cavity QED system with many degrees of freedom, the naive scenario of enhancing the nonlinearity by the simple amplification of intracavity light field no longer holds true. Although the nonlinearity enhancement for ideal two-level systems is subject to the light-field amplification and damping rates, the whole scenario drastically changes for many-level systems with many degrees of freedom, and more comprehensive enhancement mechanism emerges. Generally, the strength of the third-order nonlinearity is dominated largely by the balance between contributions with opposite signs, namely, the contributions from ground-state-one-exciton-state transition (absorption saturation) and those from one-exciton-state-two-exciton-state transition (induced absorption). For a system with many degrees of freedom, the change in level structure, resulting from size change and/or biexciton formation, strongly modulates the above balance and the size dependence of the nonlinearity.⁸ If such a system is placed within a cavity, the exciton-cavity system in the

strong-coupling regime forms one- and two-polariton states, and their level structures are then drastically changed by the size of the exciton system. These results strongly indicate that we can control the optical nonlinearity by manipulating the level structures of cavity polaritons and biexcitons by adjusting the size and system parameters of the exciton-cavity system. In this study, we therefore demonstrate the effects of the formation of cavity polaritons and biexcitons on the size dependence of the nonlinearity; this reveals another essential function of the cavity QED to enhance the optical nonlinearity.

The rest of this paper is organized as follows. In Sec. II, we formulate an exciton-cavity system, forming cavity polaritons and biexcitons, and the optical master equation in the framework of cavity polaritons. In Sec. III, we analyze in detail the third-order nonlinear optical response of the cavity polaritons. In Sec. IV, we summarize our results.

II. THEORETICAL MODEL

As a model system, we consider an exciton-cavity system, as depicted in Fig. 1(a), where a $\lambda/2$ cavity is assumed and the exciton system is placed at the center of the cavity. Pump and probe beams are normally incident on the surface of the cavity. In this study, we focus on the signal emitted normally on the same side as the incident lights. For simplicity, in these optical processes, we ignore the nonradiative decay of excitons.

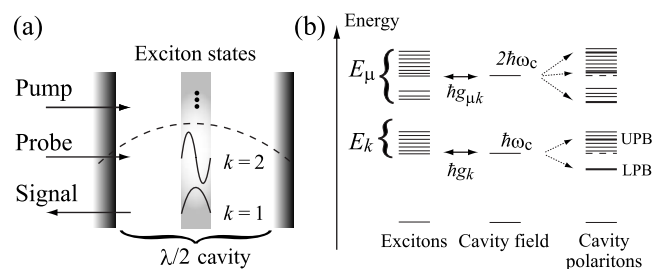


FIG. 1. Schematic of (a) pump-probe assignment and (b) formation of cavity polaritons. k and μ are the quantum numbers of one- and two-exciton states, respectively. $\hbar g$ is the exciton-cavity coupling.

The Hamiltonian for the fundamental mode of a $\lambda/2$ cavity field is given by

$$\hat{H}_C = \hbar\omega_c \hat{c}^\dagger \hat{c}, \quad (1)$$

where \hat{c} (\hat{c}^\dagger) is the annihilation (creation) operator of the cavity photon with frequency ω_c . The interaction Hamiltonian describing the exciton-cavity coupling can be written as

$$\hat{H}_{\text{int}} = \hbar \sum_k g_k (\hat{c}^\dagger \hat{b}_k + \hat{c} \hat{b}_k^\dagger), \quad (2)$$

where k is the quantum number of exciton states, g_k is the exciton-cavity coupling rate, and \hat{b}_k (\hat{b}_k^\dagger) is the exciton annihilation (creation) operator. When the exciton-cavity coupling is larger than the spontaneous emission of excitons and the cavity damping, excitons are strongly coupled with cavity photons, and they form the so-called cavity polaritons [Fig. 1(b)].

For the exciton system, as a first step, we adopt a one-dimensional discrete-lattice model of an exciton because it provides tractable solutions of bound and unbound two-exciton states as a complete set. Further, we ignore the spin degree of freedom of excitons. This model is sufficient to demonstrate the qualitative aspects of the essential physics of this study.⁹ The Hamiltonian of the exciton system can be described as¹⁰

$$\hat{H}_X = \epsilon \sum_\ell \hat{b}_\ell^\dagger \hat{b}_\ell - t \sum_\ell (\hat{b}_{\ell+1}^\dagger \hat{b}_\ell + \hat{b}_\ell^\dagger \hat{b}_{\ell+1}) - \Delta \sum_\ell \hat{b}_\ell^\dagger \hat{b}_{\ell+1}^\dagger \hat{b}_{\ell+1} \hat{b}_\ell, \quad (3)$$

where b_ℓ (b_ℓ^\dagger) is the exciton annihilation (creation) operator at the ℓ th site, ϵ is the excitation energy of each site, and t is the transfer energy of an exciton from a site to neighboring sites. The last term is the attractive interaction between two neighboring excitons, leading to the biexciton formation. With the boundary condition that the exciton states are zero at sites $\ell=0$ and $\ell=N+1$, the eigenenergy and eigenstate for the one-exciton state are, respectively, given by

$$E_k = \epsilon - 2t \cos ka, \quad (4)$$

$$|k\rangle = \sqrt{\frac{2}{N+1}} \sum_\ell \sin(k\ell a) \hat{b}_\ell^\dagger |0\rangle, \quad (5)$$

where a is the lattice constant and N is the size of the exciton system. Eigenstates for a two-exciton state can be written as $|\mu\rangle = \sum_{\ell < m} C_{\ell,m}^{(\mu)} |\ell, m\rangle$, where $|\ell, m\rangle \equiv |\ell\rangle \otimes |m\rangle$ and the states of $|m, m\rangle$ for any m are excluded. This prohibition of two excitons occupying the same site corresponds to the Pauli exclusion principle. The coefficients $C_{\ell,m}^{(\mu)}$ are numerically calculated and determined, so that $\{|\mu\rangle\}_\mu$ forms a complete system. The biexciton binding energy is then uniquely determined by t and Δ . In particular, the binding energy of the biexciton with the lowest energy is denoted by Δ_B . The k representation of $|\mu\rangle$ is obtained simply by Fourier transforming $C_{\ell,m}^{(\mu)}$ to $C_{k,k'}^{(\mu)}$.

The eigenstates of the exciton-cavity system can now be obtained by diagonalizing the Hamiltonian $\hat{H}_{\text{sys}} = \hat{H}_X + \hat{H}_C$

+ \hat{H}_{int} . Rewriting the exciton operator \hat{b}_k using the Hubbard operators as¹¹

$$\hat{b}_k = |G\rangle\langle k| + \sum_{k'} \langle k' | \hat{b}_k | k, k'\rangle |k'\rangle\langle k, k'| + \dots, \quad (6)$$

the eigenstates can be expressed, in form, as

$$|1p\rangle^\pm = \alpha_x |k; 0\rangle \pm \alpha_c |G; 1\rangle, \quad (7)$$

$$|2p\rangle = \alpha_{xx} |k, k'; 0\rangle + \alpha_{xc} |k; 1\rangle + \alpha_{cc} |G; 2\rangle, \quad (8)$$

where $|G\rangle$ is the ground state and the separation by a semicolon denotes |exciton; photon>. $|1p\rangle^-$ is the lower cavity-polariton branch (LPB) and $|1p\rangle^+$ is the upper cavity-polariton branch (UPB). $|2p\rangle$ is the two-cavity-polariton state consisting of the two-exciton state $|k, k'; 0\rangle$, the one-exciton-one-photon state $|k; 1\rangle$, and the two-photon state $|G; 2\rangle$. In this study, we consider the third-order nonlinear optical response of cavity polaritons and therefore cavity-polariton states up to $|2p\rangle$ are required. $\hbar g_k$ is dependent on N through the dipole transition matrix of an exciton $\sum_\ell \langle G | \hat{b}_\ell | k\rangle$ and is proportional to $\sum_\ell \langle G | \hat{b}_\ell | k\rangle \cdot \hbar g_{\mu k}$ for $|2p\rangle$ can be calculated from $\hbar g_{\mu k} = \langle k; 1 | \hat{H}_{\text{int}} | \mu; 0\rangle$.

The nonlinear optical response of the exciton-cavity system can be analyzed by using the optical master equation and the input-output theory. The master equation is given by

$$\begin{aligned} \frac{d\hat{\rho}}{dt} = & \frac{1}{i\hbar} [\hat{H}_{\text{sys}} + \hat{H}_{\text{ext}}, \hat{\rho}] + \kappa (2\hat{c}^\dagger \hat{\rho} \hat{c} - \hat{c}^\dagger \hat{c} \hat{\rho} - \hat{\rho} \hat{c}^\dagger \hat{c}) \\ & + \sum_k \gamma (2\hat{b}_k^\dagger \hat{\rho} \hat{b}_k - \hat{b}_k^\dagger \hat{b}_k \hat{\rho} - \hat{\rho} \hat{b}_k^\dagger \hat{b}_k), \end{aligned} \quad (9)$$

where κ is the cavity damping rate and γ is the spontaneous emission rate of excitons into noncavity modes. \hat{H}_{ext} is the interaction Hamiltonian between intracavity photons and classical cw lights, $\xi_{\text{pump}}(t)$ and $\xi_{\text{probe}}(t)$, given by

$$\hat{H}_{\text{ext}} = i\hbar \sqrt{2\kappa} [\xi_{\text{pump}}(t) + \xi_{\text{probe}}(t)] + \text{H.c.} \quad (10)$$

Considering \hat{H}_{ext} as a perturbation term, we calculate the third-order density operator of $\rho^{(3)}$. As is well known, the optical nonlinearity is evaluated by the susceptibility χ . In exciton-cavity systems, however, there is no counterpart of χ . Therefore, we directly evaluate the third-order output field by using the input-output theory. According to the input-output theory,¹² the third-order output field can be described as

$$\xi_{\text{output}}^{(3)} = \sqrt{2\kappa} \text{Tr}[\hat{c} \hat{\rho}^{(3)}]. \quad (11)$$

In the pump-probe calculation, the pump energy is tuned to the LPB.

III. RESULTS

In this section, we analyze the third-order nonlinear optical response of cavity polaritons. First, we calculate the eigenenergies of one-cavity-polariton states and two-cavity-polariton states in terms of the dependence on exciton system

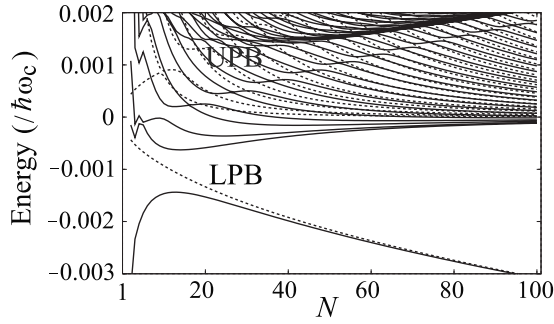


FIG. 2. E_{1p} and E_{2p} as functions of N . The solid lines indicate $E_{2p} - \hbar\omega_c - \text{LPB}$ and the dashed lines indicate $E_{1p} - \hbar\omega_c$. The exciton parameters are $t/\hbar\omega_c = 0.0033$ and $\Delta_B/\hbar\omega_c = 0.00133$. $\hbar g$ is set to $g_1/\omega_c = 0.0005$ at $N=2$.

size. Second, we calculate the third-order nonlinear optical response of cavity polaritons for different system sizes and show that the level-structure change in cavity polaritons strongly affects the nonlinear strength and there exists an optimal size of exciton system where the nonlinear strength is maximal. Finally, we discuss the enhancement mechanism of nonlinearity at the optimal size of the exciton system.

Figure 2 shows the eigenenergies E_{1p} for $|1p\rangle$ and E_{2p} for $|2p\rangle$ as functions of N . The vertical axes are expressed so as to correspond to the probe energy, $(\omega_{\text{probe}} - \omega_c)/\omega_c$. The exciton parameters are $t/\hbar\omega_c = 0.0033$ and $\Delta_B/\hbar\omega_c = 0.00133$, so that we can discuss the convergence of exciton states for relatively small N . $\hbar g_k$ is set to $g_1/\omega_c = 0.0005$ at $N=2$. There is a large difference between the level structures of $1p$ and $2p$ states, especially near the LPB for small N . This large difference mainly arises from two factors. One is the change in the level structure of two-exciton states owing to the biexciton formation. In particular, for small N , two-exciton states are sparsely distributed and the biexciton binding energy changes with N . As a result, the level structure of two-exciton states is strongly affected by the size change in the region of small N . Another is the difference between exciton-cavity coupling in one- and two-exciton states, $\hbar g_k$ and $\hbar g_{\mu k}$, owing to the difference between the dipole transition matrices in these two states. The difference between the level structures changes the balance between the contributions from $|1p\rangle$ and $|2p\rangle$ states and therefore strongly affects the strength of nonlinearity.

Figure 3(a) shows the spectra of $\text{Im}[\xi^{(3)}]$ for system sizes of $N=5, 11, 21, 41$, and 81 . The calculation parameters are $\gamma/\omega_c = 0.00033$ and $\kappa/\omega_c = 0.0005$, corresponding to a quality factor of $Q=1000$, and the other parameters are the same as those in Fig. 2. For all sizes N in Fig. 3(a), one can find the positive and negative peaks. These peaks arise from the balance between the contributions from ground-state- $1p$ -state transitions and those from $1p$ -state- $2p$ -state transitions. The negative contributions to $\text{Im}[\xi^{(3)}]$ are due to the absorption saturation in the ground-state- $1p$ -state transition and the positive contributions to $\text{Im}[\xi^{(3)}]$ are due to the induced absorption in the $1p$ -state- $2p$ -state transition. As a result of the balance of these contributions, the nonlinear strength and spectral shape of $\text{Im}[\xi^{(3)}]$ are intricately determined. The dominant peaks

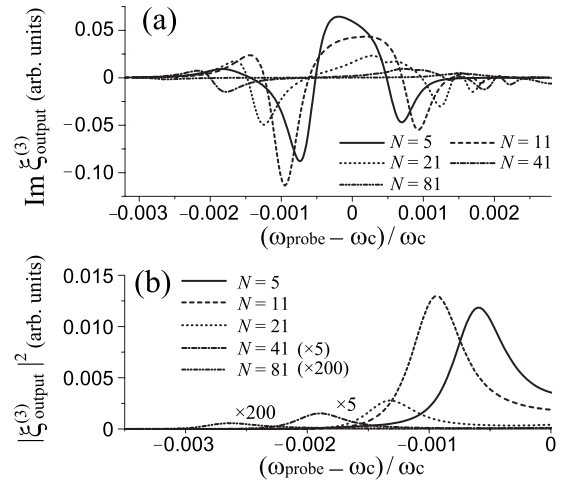


FIG. 3. (a) $\text{Im}[\xi^{(3)}]$ and (b) $|\xi^{(3)}|^2$ for $N=5, 11, 21, 41$, and 81 . The cavity QED parameters are $g_1/\omega_c = 0.0005$ (for $N=2$), $\kappa/\omega_c = 0.0005$ ($Q=1000$), and $\gamma/\omega_c = 0.000166$. The other parameters are the same as those in Fig. 2.

are the negative peaks from the LPB at ≈ -0.001 and the UPB at ≈ 0.001 ; these peaks are maximized near the LPB. The spectra of $|\xi^{(3)}|^2$ near the LPB are shown in Fig. 3(b). As N increases, the Rabi splitting gradually broadens and the peak height changes. With the present parameters, the nonlinear strength becomes maximal for $N=11$ and drastically decreases for a further increase in N . In particular, the nonlinear strength for $N=81$ decreases by a factor of 10^{-3} as compared to that for $N=11$. This result implies that there exists an optimal size of the exciton system for the given parameters, where the optical nonlinearity of the cavity polaritons is maximal, and that an oversized exciton system leads to a drastic decrease in the optical nonlinearity.

For a given set of parameters, there is thus a specific system size of excitons, where the nonlinear strength is maximal. Figure 4(a) shows the maximal strength $|\xi^{(3)}|_{\text{max}}^2$ obtained near the LPB as a function of N for several values of Δ_B . The calculation parameters except Δ_B are the same as those in Fig. 3. As Δ_B increases, the size dependence of $|\xi^{(3)}|_{\text{max}}^2$ changes, and the local maximum, corresponding to an optimal size, gradually increases (indicated by arrows). For comparison, $|\xi^{(3)}|_{\text{max}}^2$ for $\Delta_B=0$ (without biexcitons) is plotted with a solid line. In the absence of biexciton, the size dependence of $|\xi^{(3)}|_{\text{max}}^2$ is qualitatively the same as the results of Ref. 4, and for $N \gg 1$ it gradually and monotonically decreases to zero. Intriguingly, $|\xi^{(3)}|_{\text{max}}^2$ for $\Delta_B=0$ can be larger than $|\xi^{(3)}|_{\text{max}}^2$ obtained from biexcitons with small Δ_B for large N . The biexciton with small Δ_B thus adversely decreases the optical nonlinearity, as a result of the balance between the contributions from the absorption saturation and induced absorption. Figure 4(b) shows the dependence of $|\xi^{(3)}|_{\text{max}}^2$ on N for several values of γ , where Δ_B is constant. The increase in γ leads to a decrease in the optical nonlinear strength as well as of the optimal system size of excitons (indicated by arrow). The main effect of γ on decrease in nonlinearity is then to balance out the contributions from the absorption saturation and induced absorption, which is more likely caused by a broadened linewidth. In practice, both Δ_B

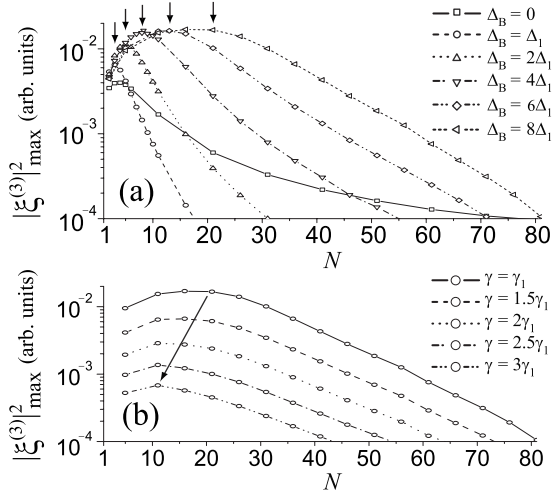


FIG. 4. Dependence of $|\xi^{(3)}|_{\max}^2$ on N for different Δ_B and γ . (a) $\gamma = \gamma_1$ and Δ_B is variable and (b) $\Delta_B = 8\Delta_1$ and γ is variable, where $\gamma_1 \equiv 0.000\ 166\hbar\omega_c$ and $\Delta_1 \equiv 0.001\ 33\hbar\omega_c$. The other parameters are the same as those in Fig. 3.

and γ concurrently affect the size dependence of the optical nonlinearity. Since a typical size of the lattice constant is $a \approx 0.5$ nm, our results indicate that a size difference of a few nanometers and a slight difference of the parameters might lead to a decrease in the nonlinear strength by a factor of 10^{-1} . Thus, the exciton-cavity parameters modify the balance between the contributions from absorption saturation and induced absorption, and this leads to a drastic change in the size dependence of the optical nonlinearity. Therefore, to educe the strong optical nonlinearities of the exciton-cavity system, especially the biexciton nonlinearity, careful control of the exciton-cavity parameters is required.

Finally, we discuss the enhancement mechanism of nonlinearity at an optimal size of the exciton system. In the previous studies, we have clarified that efficient biexciton-cavity coupling can be achieved at the level anticrossing of a biexciton and cavity polaritons, where a cavity bipolariton state is formed by a superposition state of a biexciton and two-cavity polaritons described, in form, as^{6,7} $|2p\rangle \approx |B\rangle \pm (|k, k'; 0\rangle + |k; 1\rangle + |G; 2\rangle)$, where $|B\rangle$ is the biexciton state. This means that the biexciton remains almost bare and is weakly coupled with cavity photons through the cavity polaritons. It is known that the cavity bipolariton is stable only for $\hbar g \sim \Delta_B$. The dependence of Δ_B and $2\hbar g_1$ on N is shown in Fig. 5. The intersections of Δ_B and $2\hbar g_1$ are in good agreement with the optimal sizes shown in Fig. 4(a), and the level anticrossings are realized at these points,¹³ as can be seen near the LPB at $N=11$ in Fig. 2(b). Owing to the level anticrossing, the overlap of energy levels between the cavity bipolariton and the LPB becomes small and thus their contributions cannot balance out. As a result, the maximal nonlinearity can be achieved. The realization of maximal nonlinearity in the biexciton-cavity coupling can thus be reduced to the realization of the cavity bipolariton with level anticrossing. If the level anticrossing points for larger N are required, we have only to achieve a small dipole transition $\Sigma_\ell \langle G | \hat{b}_\ell | k \rangle$, so that the curve of $2\hbar g_1$ becomes gradual and

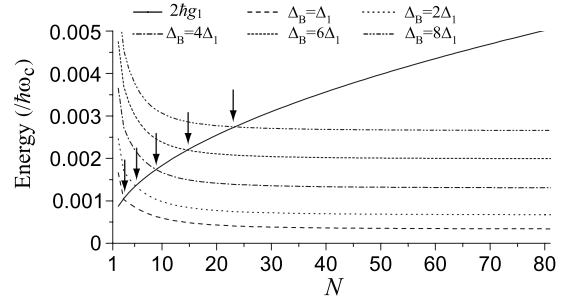


FIG. 5. Dependence of Δ_B and $2\hbar g_1$ on N . The calculation parameters except Δ_B are the same as those in Fig. 2.

the intersections of Δ_B and $2\hbar g_1$ shift to larger N . This can be achieved by selecting a material in which the transition between $|G\rangle$ and $|k\rangle$ is very small or almost forbidden.⁵

IV. CONCLUSIONS AND DISCUSSION

In conclusion, we have theoretically investigated the third-order nonlinear optical response of cavity polaritons in terms of the size dependence of the exciton system and revealed that the control of the balance between the contributions from the absorption saturation and induced absorption is another essential function of the cavity QED in order to enhance the optical nonlinearity. The size dependence of the nonlinearity can be drastically changed by a slight difference of the exciton-cavity parameters, especially Δ_B and γ . We have shown that there exists a specific size of the exciton system, characterized by $\Delta_B \approx 2\hbar g$, where the maximal nonlinear strength is realized.

Throughout this work, we have focused on especial parameters so as to show the convergence of exciton states for relatively small N . Here we provide and discuss two real systems, as examples, in which the obtained results can be implemented. The first is the excitons in bundled J aggregates, such as Langmuir-Blodgett film, confined in a microcavity. J aggregates can be treated as a one-dimensional Frenkel-type exciton system, and therefore our model is directly applicable. In fact, cavity polaritons formed in J aggregates have been investigated.¹⁴ To our knowledge, stable biexcitons in J aggregates have not been reported; therefore, relatively small size of J aggregates would be useful to enhance the optical nonlinearity of cavity polariton.

Another is the excitons in a quantum well confined in a microcavity, if we focus on a zero center-of-mass motion of two-exciton states, with the extension of our model appropriately including the relative in-plane motions of the two constituent excitons. In particular, spectra of CuCl thin films are well reproduced by the tight-binding exciton model discussed in this work. CuCl has a biexciton with large binding energy ($\Delta_B \approx 30$ meV), and recently a giant Rabi splitting of $2\hbar g \sim 100$ meV has been experimentally observed in CuCl microcavity.¹⁵ If the exciton-cavity system can be designed so as to realize $\Delta_B \approx 2\hbar g$, the strong enhancement of optical nonlinearity due to the level anticrossing could be expected.

The size dependence of nonlinearity might be more drastically changed by the dimension of the exciton system, and

therefore further analyses of higher-dimensional system would be interesting. We hope that the results in this study help to identify some of the practical requirements for an optimal exciton system size.

ACKNOWLEDGMENTS

We thank A. Ishikawa for his helpful discussion. This

work was supported by a Grant-in-Aid for Creative Scientific Research (No. 17GS1204) from the Japan Society for the Promotion of Science and KAKENHI (Grant-in-Aid for Scientific Research) on Priority Area “Strong Photons-Molecules Coupling Fields” (No. 470) from the Ministry of Education, Culture, Sports, Science and Technology of Japan.

-
- ¹K. M. Birnbaum, A. Boca, R. Miller, A. D. Boozer, T. E. Northup, and H. J. Kimble, *Nature (London)* **436**, 87 (2005).
- ²P. G. Savvidis, J. J. Baumberg, R. M. Stevenson, M. S. Skolnick, D. M. Whittaker, and J. S. Roberts, *Phys. Rev. Lett.* **84**, 1547 (2000).
- ³R. Houdré, C. Weisbuch, R. P. Stanley, U. Oesterle, and M. Illegems, *Phys. Rev. Lett.* **85**, 2793 (2000).
- ⁴K. Koshino and H. Ishihara, *Phys. Rev. A* **71**, 063818 (2005).
- ⁵A. Ishikawa and H. Ishihara, *Phys. Rev. Lett.* **100**, 203602 (2008).
- ⁶H. Ajiki and H. Ishihara, *J. Phys. Soc. Jpn.* **76**, 053401 (2007).
- ⁷H. Oka and H. Ishihara, *Phys. Rev. Lett.* **100**, 170505 (2008).
- ⁸H. Ishihara and T. Amakata, *Int. J. Mod. Phys. B* **15**, 3809 (2001).
- ⁹The results in this work are applicable to other more complex exciton model without loss of generality. However, the calculation will be quite complicated.
- ¹⁰H. Ishihara, T. Amakata, and K. Cho, *Phys. Rev. B* **65**, 035305 (2001).
- ¹¹Th. Östreich, K. Schönhammer, and L. J. Sham, *Phys. Rev. Lett.* **74**, 4698 (1995).
- ¹²D. F. Walls and G. J. Milburn, *Quantum Optics* (Springer, Berlin, 1994).
- ¹³For larger Δ_B (or $\hbar g$), intersections of Δ_B and $2\hbar g$ become slightly different from optimal sizes because the splitting width of level anticrossing becomes larger.
- ¹⁴See, for example, A. I. Tartakovskii, M. Emam-Ismael, D. G. Lidzey, M. S. Skolnick, D. D. C. Bradley, S. Walker, and V. M. Agranovich, *Phys. Rev. B* **63**, 121302(R) (2001).
- ¹⁵G. Oohata, T. Nishioka, D. Kim, H. Ishihara, and M. Nakayama, *Phys. Rev. B* **78**, 233304 (2008).